

## Lattice effective field theory for nuclei from $A = 4$ to $A = 28$

---

**Timo A. Lähde<sup>\*,a</sup>, Evgeny Epelbaum<sup>b</sup>, Hermann Krebs<sup>b</sup>, Dean Lee<sup>c</sup>,  
Ulf-G. Meißner<sup>ade</sup> and Gautam Rupak<sup>f</sup>**

<sup>a</sup>*Institute for Advanced Simulation, Institut für Kernphysik, and*

*Jülich Center for Hadron Physics, Forschungszentrum Jülich, D-52425 Jülich, Germany*

<sup>b</sup>*Institut für Theoretische Physik II, Ruhr-Universität Bochum, D-44870 Bochum, Germany*

<sup>c</sup>*Department of Physics, North Carolina State University, Raleigh, NC 27695, USA*

<sup>d</sup>*Helmholtz-Institut für Strahlen- und Kernphysik and Bethe Center for Theoretical Physics,  
Universität Bonn, D-53115 Bonn, Germany*

<sup>e</sup>*JARA – High Performance Computing, Forschungszentrum Jülich, D-52425 Jülich, Germany*

<sup>f</sup>*Department of Physics and Astronomy, Mississippi State University, Mississippi State,  
MS 39762, USA*

*E-mail:* t.laehde@fz-juelich.de, evgeny.epelbaum@rub.de,

hermann.krebs@rub.de, dean\_lee@ncsu.edu, u.meissner@fz-juelich.de,

grupak@u.washington.edu

We present an overview of the extension of Nuclear Lattice Effective Field Theory simulations to the regime of medium-mass nuclei. We focus on the determination of the ground-state energies of the alpha nuclei  $^{16}\text{O}$ ,  $^{20}\text{Ne}$ ,  $^{24}\text{Mg}$  and  $^{28}\text{Si}$  by means of Euclidean time projection.

PACS: 21.10.Dr, 21.30.-x, 21.60.De

*31st International Symposium on Lattice Field Theory LATTICE 2013*

*July 29 – August 3, 2013*

*Mainz, Germany*

---

\*Speaker.

## 1. Introduction

Nuclear Lattice Effective Field Theory (NLEFT) is a first-principles approach, in which Chiral EFT for nucleons is combined with numerical Auxiliary-Field Quantum Monte Carlo (AFQMC) lattice simulations. NLEFT differs from other *ab initio* methods [1–6] in that it is an unconstrained Monte Carlo calculation, which does not rely on truncated basis expansions or many-body perturbation theory, nor on prior information about the structure of the nuclear wave function.

## 2. Nuclear Lattice EFT at NNLO

As in Chiral EFT, our calculations are organized in powers of a generic soft scale  $Q$  associated with factors of momenta and the pion mass [7]. We denote  $\mathcal{O}(Q^0)$  as leading order (LO),  $\mathcal{O}(Q^2)$  as next-to-leading order (NLO), and  $\mathcal{O}(Q^3)$  as next-to-next-to-leading order (NNLO) contributions. The present calculations are performed up to NNLO. We define  $H_{\text{LO}}$  as the LO lattice Hamiltonian, and  $H_{\text{SU}(4)}$  as the equivalent Hamiltonian with the pion-nucleon coupling  $g_A = 0$  and contact interactions that respect Wigner’s SU(4) symmetry.

In our NLEFT calculations (see Ref. [8] for a review),  $H_{\text{LO}}$  is treated non-perturbatively. The NLO contribution to the two-nucleon force (2NF), the electromagnetic and strong isospin-breaking contributions (EMIB), and the three-nucleon force (3NF) which first enters at NNLO, are all treated as perturbations. It should be noted that our “LO” calculations use smeared short-range interactions that capture much of the corrections usually treated at NLO [9]. The 3NF at NNLO over-binds nuclei with  $A > 4$  due to a clustering instability which involves four nucleons on the same lattice site. The long-term objective of NLEFT is to remedy this problem by decreasing the lattice spacing and including the N3LO corrections in Chiral EFT. In the mean time, the over-binding problem has been rectified by means of a 4N contact interaction, tuned to the empirical binding energy of either  ${}^4\text{He}$  or  ${}^8\text{Be}$  [10]. While this provides a good description of the alpha nuclei up to  $A = 12$  including the Hoyle state [10–12], the over-binding is found to increase more rapidly for  $A \geq 16$ . Therefore, in Ref. [13] a non-local 4N interaction which accounts for all possible configurations of four nucleons on adjacent lattice sites was introduced, and adjusted to the empirical binding energy of  ${}^{24}\text{Mg}$ . A detailed study of the spectrum of  ${}^{16}\text{O}$  will be reported separately [14].

## 3. Euclidean time projection

The NLEFT calculations reported here (see also Ref. [13]) are performed with a (spatial) lattice spacing of  $a = 1.97$  fm in a periodic cube of length  $L = 11.8$  fm. Our trial wave function  $|\Psi_A^{\text{init}}\rangle$  is a Slater-determinant state composed of delocalized standing waves, with  $A$  nucleons and the desired spin and isospin. First, we project  $|\Psi_A^{\text{init}}\rangle$  for a time  $t'$  using the Euclidean-time evolution operator of the SU(4) Hamiltonian, giving the “trial state”  $|\Psi_A(t')\rangle \equiv \exp(-H_{\text{SU}(4)}t')|\Psi_A^{\text{init}}\rangle$ . Second, we use the full Hamiltonian  $H_{\text{LO}}$  to construct the Euclidean-time projection amplitude

$$Z_A(t) \equiv \langle \Psi_A(t') | \exp(-H_{\text{LO}}t) | \Psi_A(t') \rangle, \quad E_A(t) = -\partial[\ln Z_A(t)]/\partial t, \quad (3.1)$$

and the “transient energy”  $E_A(t)$ . If we denote by  $|\Psi_{A,0}\rangle$  the lowest (normalizable) eigenstate of  $H_{\text{LO}}$  which has a non-vanishing overlap with the trial state  $|\Psi_A(t')\rangle$ , we obtain the corresponding energy  $E_{A,0}$  as the  $t \rightarrow \infty$  limit of  $E_A(t)$ .

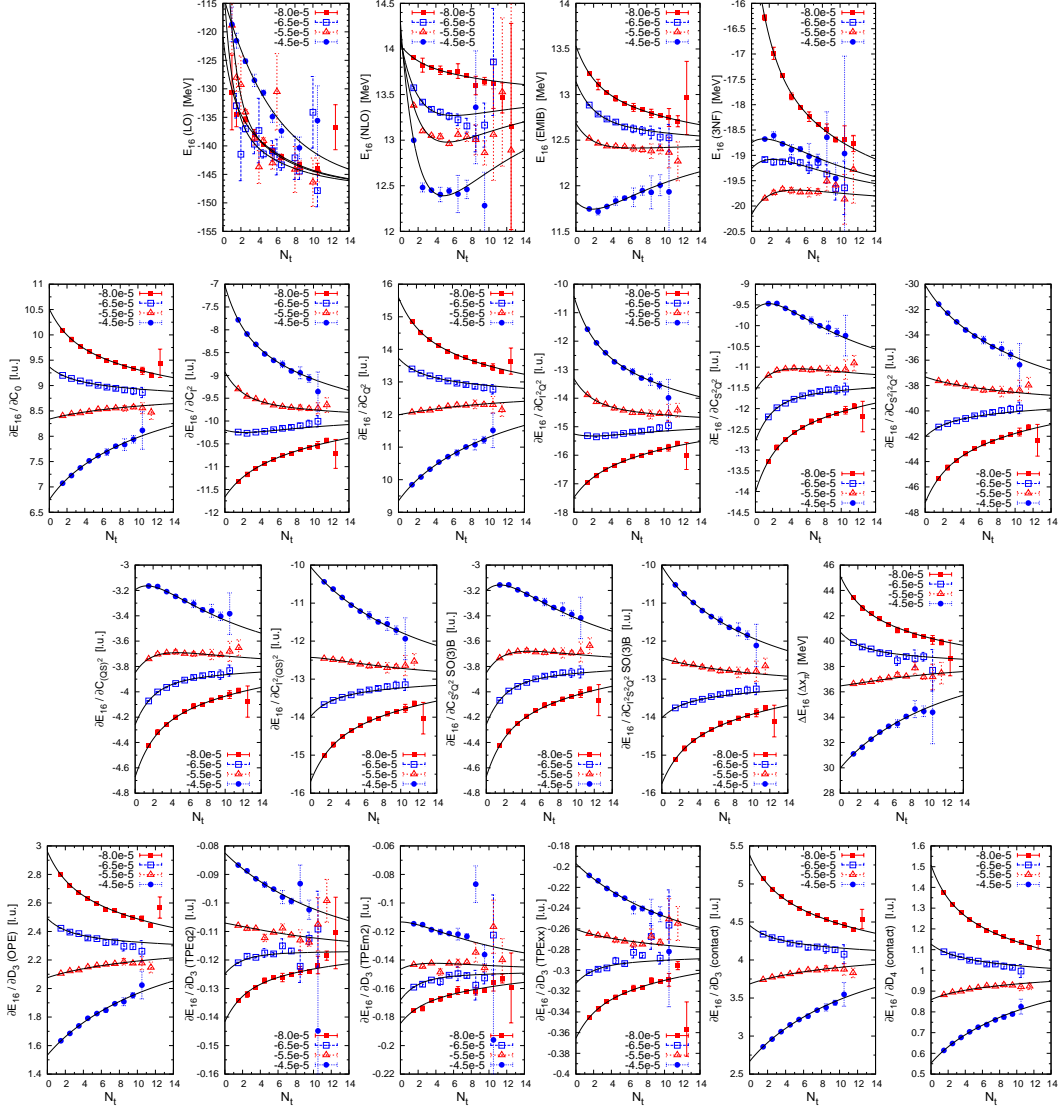


**Figure 1:** NLEFT results for  $^{16}\text{O}$ . The LO energy is  $E_{\text{LO}} = -147.3(5)$  MeV, and the result at NNLO including  $4N$  interactions is  $E_{\text{NNLO}+4N} = -131.3(5)$  MeV. The empirical binding energy is  $-127.62$  MeV.

The NLO and NNLO contributions are evaluated in perturbation theory. We compute operator expectation values using

$$Z_A^\mathcal{O}(t) \equiv \langle \Psi_A(t') | \exp(-H_{\text{LO}}t/2) \mathcal{O} \exp(-H_{\text{LO}}t/2) | \Psi_A(t') \rangle, \quad (3.2)$$

for any operator  $\mathcal{O}$ . Given the ratio  $X_A^\mathcal{O}(t) = Z_A^\mathcal{O}(t)/Z_A(t)$ , the expectation value of  $\mathcal{O}$  for the desired state  $|\Psi_{A,0}\rangle$  is obtained as  $X_{A,0}^\mathcal{O} \equiv \langle \Psi_{A,0} | \mathcal{O} | \Psi_{A,0} \rangle = \lim_{t \rightarrow \infty} X_A^\mathcal{O}(t)$ .

Sign oscillations make it difficult to reach sufficiently large values of the projection time  $t$ . It is helpful to note that the closer the trial state  $|\Psi_A(t')\rangle$  is to  $|\Psi_{A,0}\rangle$ , the less the necessary projection time  $t$ .  $|\Psi_A(t')\rangle$  can be optimized by adjusting both the  $\text{SU}(4)$  projection time  $t'$  and the strength of the coupling  $C_{\text{SU}(4)}$  of  $H_{\text{SU}(4)}$ . The accuracy of the extrapolation  $t \rightarrow \infty$  can be further improved by simultaneously incorporating data from trial states that differ in  $C_{\text{SU}(4)}$ .

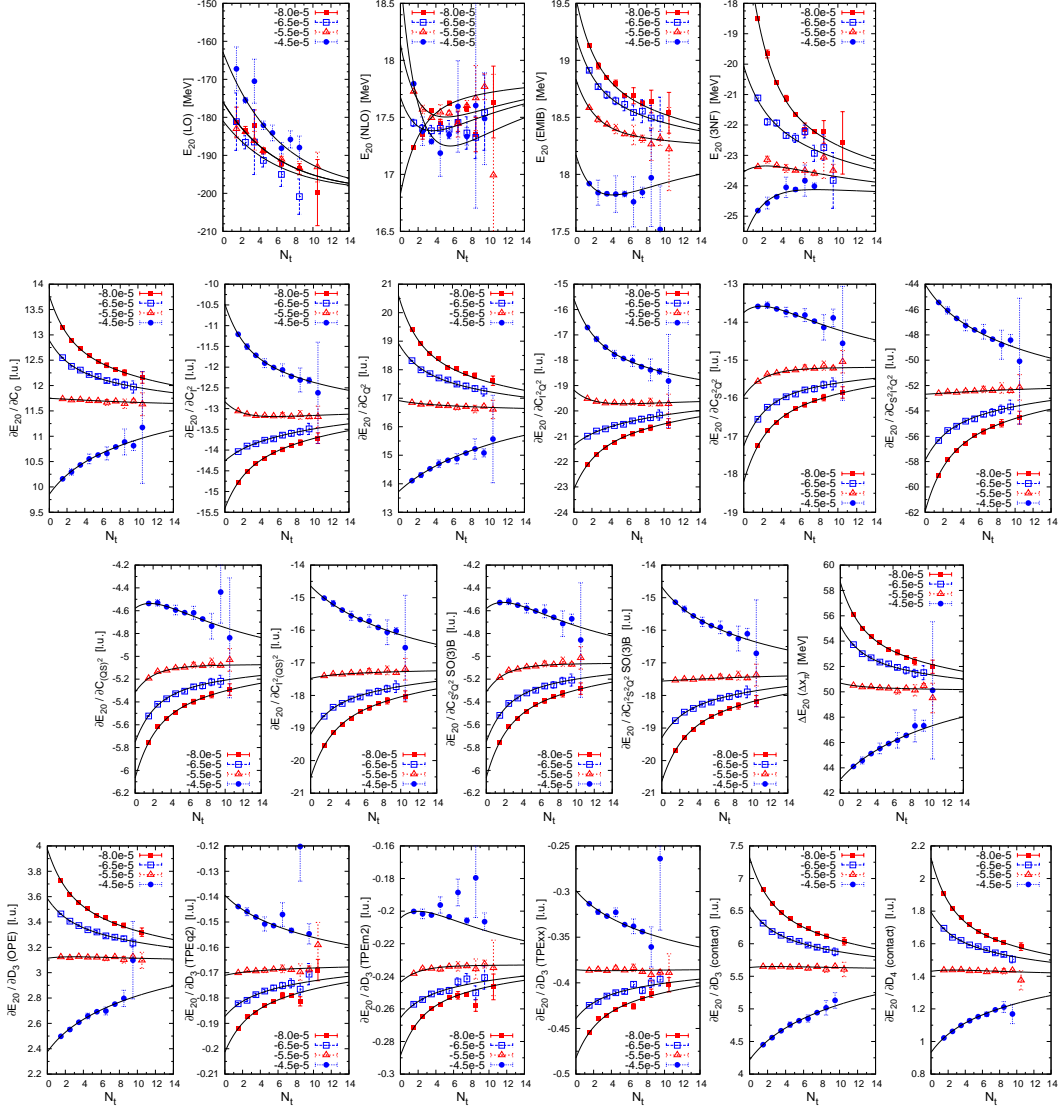


**Figure 2:** NLEFT results for  $^{20}\text{Ne}$ . The LO energy is  $E_{\text{LO}} = -199.7(9)$  MeV, and the result at NNLO including  $4N$  interactions is  $E_{\text{NNLO}+4N} = -165.9(9)$  MeV. The empirical binding energy is  $-160.64$  MeV.

The large-time behavior of  $Z_A(t)$  and  $Z_A^\theta(t)$  is controlled by the low-energy spectrum of  $H_{\text{LO}}$ . Let  $|E\rangle$  label the eigenstates of  $H_{\text{LO}}$  with energy  $E$ , and let  $\rho_A(E)$  denote the density of states for a system of  $A$  nucleons. We then express  $Z_A(t)$  and  $Z_A^\theta(t)$  in terms of their spectral representations,

$$Z_A(t) = \int dE \rho_A(E) |\langle E | \Psi_A(t') \rangle|^2 \exp(-Et), \quad (3.3)$$

$$Z_A^\theta(t) = \int dE dE' \rho_A(E) \rho_A(E') \langle \Psi_A(t') | E \rangle \langle E | \theta | E' \rangle \langle E' | \Psi_A(t') \rangle \exp(-(E + E')t/2), \quad (3.4)$$

from which we construct the spectral representations of  $E_A(t)$  and  $X_A^\theta(t)$ . We can approximate these to arbitrary accuracy over any finite range of  $t$  by taking  $\rho_A(E)$  to be a sum of energy delta functions,  $\rho_A(E) \approx \sum_{i=0}^{i_{\text{max}}} \delta(E - E_{A,i})$ , where we take  $i_{\text{max}} = 4$  for the  $^4\text{He}$  ground state, and  $i_{\text{max}} = 3$  for  $A \geq 8$ . Using data obtained for different values of  $C_{\text{SU}(4)}$ , we perform a correlated fit of  $E_A(t)$

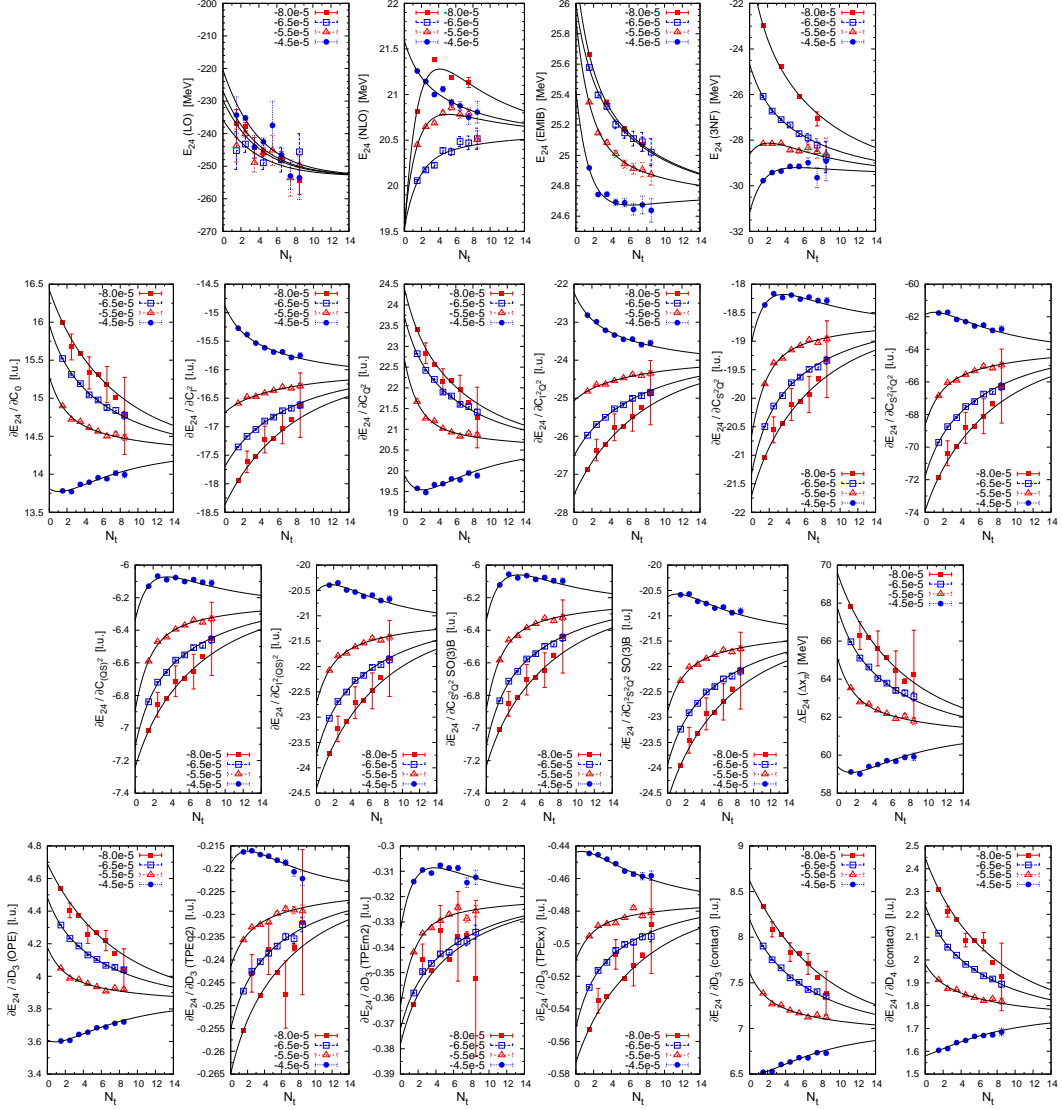


**Figure 3:** NLEFT results for  $^{24}\text{Mg}$ . The LO energy is  $E_{\text{LO}} = -253(2)$  MeV, and the result at NNLO including  $4N$  interactions is  $E_{\text{NNLO}+4N} = -198(2)$  MeV. The empirical binding energy is  $-198.26$  MeV.

and  $X_A^\mathcal{O}(t)$  for all operators  $\mathcal{O}$  that contribute to the NLO and NNLO energy corrections. We find that the use of  $2 - 6$  trial states allows for a much more precise determination of  $E_{A,0}$  and  $X_{A,0}^\mathcal{O}$  than hitherto possible. In particular, we may “triangulate”  $X_{A,0}^\mathcal{O}$  using trial states that correspond to functions  $X_A^\mathcal{O}(t)$  which converge both from above and below, thereby bracketing  $X_{A,0}^\mathcal{O}$ .

#### 4. Results

The NLEFT results for  $^{16}\text{O}$  are given in Fig. 1, for  $^{20}\text{Ne}$  in Fig. 2, for  $^{24}\text{Mg}$  in Fig. 3, and for  $^{28}\text{Si}$  in Fig. 4. The curves show a correlated fit for all trial states, using the same spectral density  $\rho_A(E)$ . The upper row in each figure shows the LO energy, the total isospin-symmetric 2NF correction (NLO), the electromagnetic and isospin-breaking corrections (EMIB) and the total

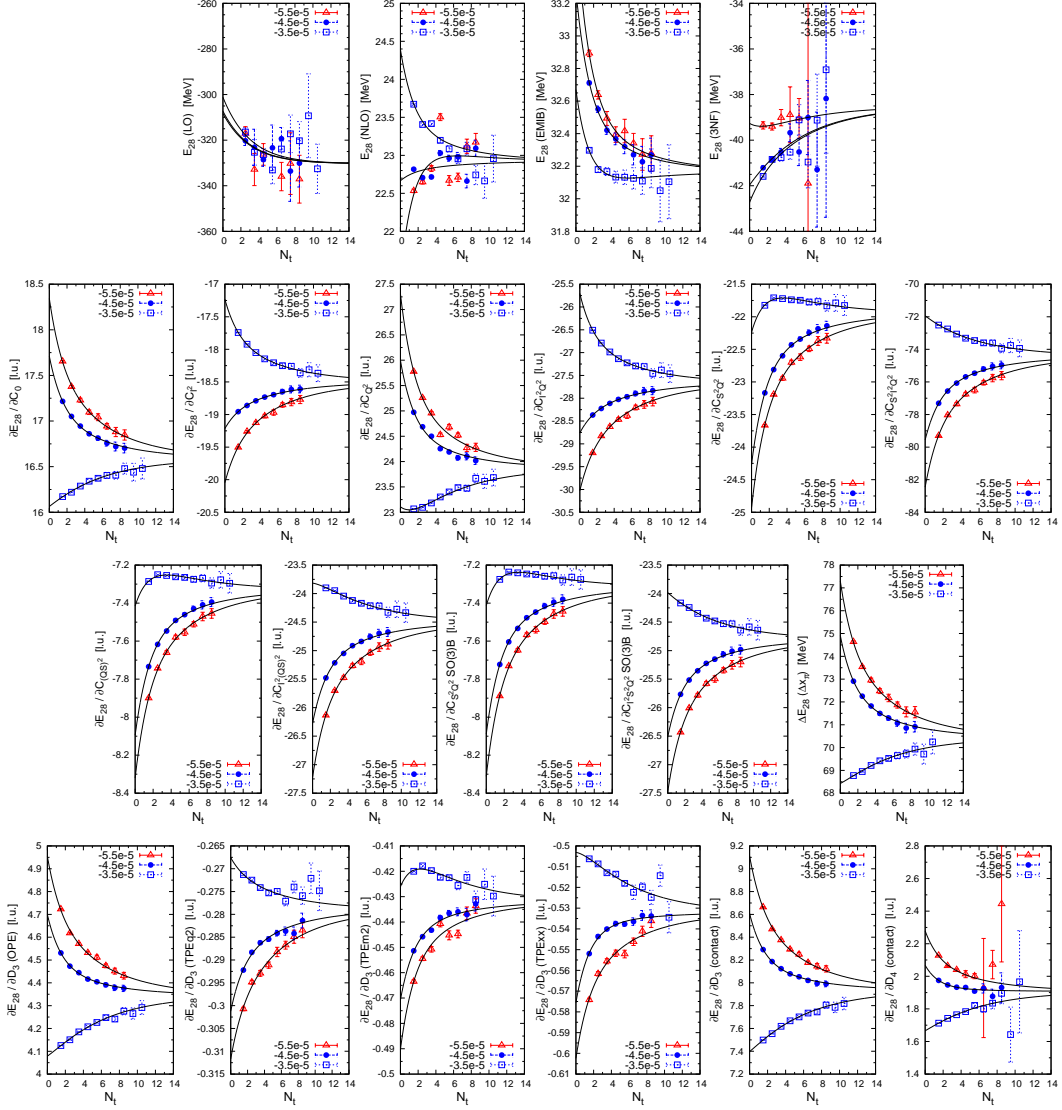


**Figure 4:** NLEFT results for  $^{28}\text{Si}$ . The LO energy is  $E_{\text{LO}} = -330(3)$  MeV, and the result at NNLO including 4N interactions is  $E_{\text{NNLO}+4\text{N}} = -233(3)$  MeV. The empirical binding energy is  $-236.54$  MeV.

3NF correction. The remaining panels show the matrix elements  $X_A^\theta(t)$  that form part of the NLO and 3NF terms. The operators  $\partial E_A / \partial C_i$  give the contributions of the NLO contact interactions, and  $\Delta E_A(\Delta x_\pi)$  denotes the energy shift due the  $\mathcal{O}(a^2)$ -improved pion-nucleon coupling. The operators  $\partial E_A / \partial D_i$  give the individual contributions to the total 3NF correction.

To summarize, we have reported on the extension of NLEFT to the regime of medium-mass nuclei. While the NNLO results are good up to  $A = 12$ , an increasing over-binding (associated with the momentum-cutoff scale and neglected higher-order contributions) manifests itself for  $A \geq 16$ . While the long-term objectives of NLEFT are to decrease the lattice spacing and include higher orders in the EFT expansion, we also find that the missing physics can be approximated by an effective 4N interaction. The current exploratory results represent an important step towards more comprehensive NLEFT simulations of medium-mass nuclei in the future.

## Acknowledgments

We are grateful for the help in automated data collection by Thomas Luu. Partial financial support from the Deutsche Forschungsgemeinschaft (Sino-German CRC 110), the Helmholtz Association (Contract No. VH-VI-417), BMBF (Grant No. 06BN9006), and the U.S. Department of Energy (DE-FG02-03ER41260) is acknowledged. This work was further supported by the EU HadronPhysics3 project, and funds provided by the ERC Project No. 259218 NUCLEAREFT. The computational resources were provided by the Jülich Supercomputing Centre at the Forschungszentrum Jülich and by RWTH Aachen.

## References

- [1] G. Hagen, M. Hjorth-Jensen, G. R. Jansen, R. Machleidt, and T. Papenbrock, *Evolution of shell structure in neutron-rich calcium isotopes*, *Phys. Rev. Lett.* **109**, 032502 (2012).
- [2] E. D. Jurgenson *et al.*, *P-shell nuclei using Similarity Renormalization Group evolved three-nucleon interactions*, *Phys. Rev. C* **87**, 054312 (2013).
- [3] R. Roth, J. Langhammer, A. Calci, S. Binder, and P. Navratil, *Similarity-Transformed Chiral  $NN+3N$  Interactions for the Ab Initio Description of 12-C and 16-O*, *Phys. Rev. Lett.* **107**, 072501 (2011).
- [4] H. Hergert *et al.*, *In-Medium Similarity Renormalization Group with Chiral Two- Plus Three-Nucleon Interactions*, *Phys. Rev. C* **87**, 034307 (2013).
- [5] A. Lovato *et al.*, *Charge form factor and sum rules of electromagnetic response functions in Carbon-12*, *Phys. Rev. Lett.* **111**, 092501 (2013).
- [6] V. Somà, C. Barbieri, and T. Duguet, *Ab initio Gorkov-Green's function calculations of open-shell nuclei*, *Phys. Rev. C* **87**, 011303(R) (2013).
- [7] E. Epelbaum, H.-W. Hammer, and Ulf-G. Meißner, *Modern Theory of Nuclear Forces*, *Rev. Mod. Phys.* **81**, 1773 (2009).
- [8] D. Lee, *Lattice simulations for few- and many-body systems*, *Prog. Part. Nucl. Phys.* **63**, 117 (2009).
- [9] B. Borasoy, E. Epelbaum, H. Krebs, D. Lee, and Ulf-G. Meißner, *Lattice Simulations for Light Nuclei: Chiral Effective Field Theory at Leading Order*, *Eur. Phys. J. A* **31**, 105 (2007).
- [10] E. Epelbaum, H. Krebs, D. Lee, and Ulf-G. Meißner, *Lattice effective field theory calculations for  $A = 3, 4, 6, 12$  nuclei*, *Phys. Rev. Lett.* **104**, 142501 (2010); *ibid.*, *Lattice calculations for  $A = 3, 4, 6, 12$  nuclei using chiral effective field theory*, *Eur. Phys. J. A* **45**, 335 (2010).
- [11] E. Epelbaum, H. Krebs, D. Lee, and Ulf-G. Meißner, *Ab initio calculation of the Hoyle state*, *Phys. Rev. Lett.* **106**, 192501 (2011).
- [12] E. Epelbaum, H. Krebs, T. A. Lähde, D. Lee, and Ulf-G. Meißner, *Structure and rotations of the Hoyle state*, *Phys. Rev. Lett.* **109**, 252501 (2012); *ibid.*, *Viability of carbon-based life as a function of the light quark mass*, *Phys. Rev. Lett.* **110**, 112502 (2013); *ibid.*, *Dependence of the triple-alpha process on the fundamental constants of nature*, *Eur. Phys. J. A* **49**, 82 (2013).
- [13] T. A. Lähde, E. Epelbaum, H. Krebs, D. Lee, Ulf-G. Meißner, and G. Rupak, *Lattice Effective Field Theory for Medium-Mass Nuclei* [arXiv:1311.0477 [nucl-th]].
- [14] E. Epelbaum, H. Krebs, T. A. Lähde, D. Lee, Ulf-G. Meißner, and G. Rupak, *in preparation*.